Supramolecular Architecture in Langmuir and Langmuir−Blodgett Films Incorporating a Chiral Azobenzene

ARTICLE *in* LANGMUIR · OCTOBER 2008

Impact Factor: 4.46 · DOI: 10.1021/la801299a · Source: PubMed

6 AUTHORS, INCLUDING:

Marta Haro
Universitat Jaume I
58 PUBLICATIONS **478** CITATIONS
SEE PROFILE

Luis Oriol
University of Zaragoza
126 PUBLICATIONS **2,064** CITATIONS
SEE PROFILE

M. C. López
University of Zaragoza
98 PUBLICATIONS **1,159** CITATIONS
SEE PROFILE

Langmuir

Article

Supramolecular Architecture in Langmuir and Langmuir#Blodgett Films Incorporating a Chiral Azobenzene

Marta Haro, Jesu#s del Barrio, Ana Villares, Luis Oriol, Pilar Cea, and M. Carmen Lo#pez

Langmuir, **2008**, 24 (18), 10196-10203 • DOI: 10.1021/la801299a • Publication Date (Web): 08 August 2008

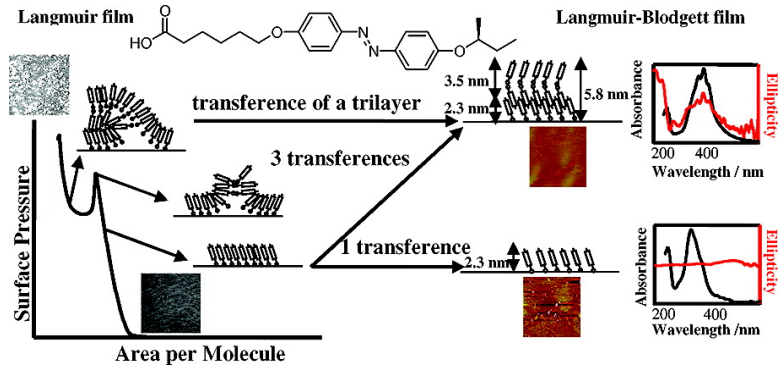

More About This Article

Additional resources and features associated with this article are available within the HTML version:

- Supporting Information
- Access to high resolution figures
- Links to articles and content related to this article
- Copyright permission to reproduce figures and/or text from this article

View the Full Text HTML

Supramolecular Architecture in Langmuir and Langmuir−Blodgett Films Incorporating a Chiral Azobenzene

Marta Haro,[†] Jesús del Barrio,[†,‡] Ana Villares,[†] Luis Oriol,[†,‡] Pilar Cea,[†,§] and M. Carmen López*[,†,§]

Departamento de Química Orgánica-Química Física, Facultad de Ciencias, Universidad de Zaragoza, Plaza de San Francisco, Ciudad Universitaria, 50009 Zaragoza, Spain, Grupo de Cristales Líquidos y Polímeros, Química Orgánica, Facultad de Ciencias, Instituto de Ciencia de Materiales de Aragón, Universidad de Zaragoza-CSIC, Pedro Cerbuna 12, 50009 Zaragoza, Spain, and Instituto de Investigación en Nanociencia de Aragón (INA), Ciudad Universitaria, 50009 Zaragoza, Spain

Received April 26, 2008. Revised Manuscript Received June 26, 2008

This article describes the synthesis and fabrication of Langmuir and Langmuir−Blodgett (LB) films incorporating a chiral azobenzene derivative, namely, (*S*)-4-*sec*-butyloxy-4′-[5″-(methyloxycarbonyl)pentyl-1″-oxy]azobenzene, abbreviated as AZO-C4(S). Appropriate conditions for the fabrication of monolayers of AZO-C4(S) at the air−water interface have been established, and the resulting Langmuir films have been characterized by a combination of surface pressure and surface potential versus area per molecule isotherms, Brewster angle microscopy, and UV−vis reflection spectroscopy. The results indicate the formation of an ordered trilayer at the air−water interface with UV−vis reflection spectroscopy showing a new supramolecular architecture for multilayered films as well as the formation of J aggregates. Films were transferred onto solid substrates, with AFM revealing well-ordered multilayered films without 3D defects. Infrared and UV−vis absorption spectroscopy indicate that the supramolecular architecture may be favored by the formation of H bonds between acid groups in neighboring layers and $\pi-\pi$ intermolecular interactions. Circular dichroism spectra reveal chiro-optical activity in multilayered LB films.

Introduction

The development of new organic components with improved electrical and optical properties is of great interest because of the growing social demand for smaller, lighter, quicker, and more efficient devices. This requires extensive experimental and theoretical investigations related to the chemistry of materials and design control of molecular and supramolecular architecture. In this context, a significant effort is being made in the investigation of the synthesis, characterization, and assembly processes of photoactive systems.[1−3] Azobenzenes are one of the most fascinating subsets of materials at the forefront of the chemistry related to photoactive components.[4−11] They are characterized by intense color, high thermal stability, photochemically induced trans−cis isomerization, and π delocalization.[4,12] Recently, the possibility of controlling supramolecular chirality in azobenzene systems upon irradiation has received much attention because of its potential application in nanometer-scale machinery, data storage, chiro-optical switches, optical devices, and molecular recognition processes.[13−20]

The fabrication of molecular assemblies to produce well-defined structures on the nanoscale can be carried out via different techniques such as self-assembly and layer by layer.[21] Among these techniques, the Langmuir−Blodgett (LB) method has the advantage of providing a good platform on which to construct supramolecular assemblies because the orientation and packing of the molecules can be arranged in a controlled manner at the air−water interface.[22−27] These ordered monolayers (Langmuir films) can be transferred from the water surface onto a solid substrate (LB films), maintaining a high order in each layer. The LB technique has been proved to be well suited to the fabrication of mono- and multilayered structured films incorporating

* To whom correspondence should be addressed. E-mail: mcarmen@unizar.es. Phone: + 34 976 76 11 96. Fax: + 34 976 76 12 02.

[†] Departamento de Química Orgánica-Química Física, Universidad de Zaragoza and Ciudad Universitaria.

[‡] Instituto de Ciencia de Materiales de Aragón, Universidad de Zaragoza-CSIC.

[§] Instituto de Investigación en Nanociencia de Aragón (INA), Ciudad Universitaria.

(1) Willner, I.; Willner, B. *J. Mater. Chem.* **1998**, *8*, 2543.
(2) Shibaev, V. P.; Bobrovsky, A. Y.; Boiko, N. I. *Prog. Polym. Sci.* **2003**, *28*, 729.
(3) Balzani, V.; Credi, A.; Venturi, M. *Molecular Devices and Machines: A Journey into the Nanoworld*. Wiley-VCH: Weinhein, Germany, 2003.
(4) Xie, S.; Natansohn, A.; Rochon, P. *Chem. Mater.* **1993**, *5*, 403.
(5) Ichimura, K. *Chem. Rev.* **2000**, *100*, 1847.
(6) Feringa, B. L.; van Delden, R. A.; Koumura, N.; Geertsema, E. M. *Chem. Rev.* **2000**, *100*, 1789.
(7) Natansohn, A.; Rochon, P. *Chem. Rev.* **2002**, *102*, 4139.
(8) Halabieh, R. H.; Mermut, O.; Barret, C. J. *Pure Appl. Chem.* **2004**, *76*, 1445.
(9) Yesodha, S. K.; Sadashiva, P.; Chennakattu, K.; Tsutsumi, N. *Prog. Polym. Sci.* **2004**, *29*, 45.
(10) Oliveira, O. N., Jr.; Dos Santos, D. S., Jr.; Balogh, D. T.; Zucolotto, V.; Mendonca, C. R. *Adv. Colloid Interface Sci.* **2005**, *116*, 179.
(11) Kay, E. R.; Leigh, D. A.; Zerbetto, F. *Angew. Chem., Int. Ed.* **2007**, *46*, 72.
(12) Sudesh Kumar, G.; Neckers, D. C. *Chem. Rev.* **1989**, *89*, 1915.
(13) Guerrero, L.; Smart, O. S.; Woolley, G. A.; Allemann, R. K. *J. Am. Chem. Soc.* **2005**, *127*, 15624.
(14) Kurihara, S.; Nomiyama, S.; Nonaka, T. *Chem. Mater.* **2000**, *12*, 9.
(15) Painelli, A.; Terenziani, F.; Angiolini, L.; Benelli, T.; Giorgini, L. *Chem.−Eur. J.* **2005**, *11*, 6053.
(16) Mitsuoka, T.; Sato, H.; Yoshida, J.; Yamagishi, A.; Einaga, Y. *Chem. Mater.* **2006**, *18*, 3442.
(17) Tejedor, R. M.; Millaruelo, M.; Oriol, L.; Serrano, J. L.; Alcalá, R.; Rodríguez, F. J.; Villacampa, B. *J. Mater. Chem.* **2006**, *16*, 1674.
(18) Khan, A.; Hecht, S. *Chem.−Eur. J.* **2006**, *12*, 4764.
(19) Guo, P.; Zhang, L.; Liu, M. *Adv. Mater.* **2006**, *18*, 177.
(20) Haruta, O.; Ijiro, K. *J. Nanosci. Nanotechnol.* **2007**, *7*, 734.
(21) Ulman, A. *An Introduction to Ultrathin Organic Films: From Langmuir-Blodgett to Self-Assembly*. Academic Press: San Diego, 1991.
(22) Nuckolls, C.; Katz, T. J.; Verbiest, T.; Van Elschocht, S.; Kuball, H.-G.; Kiesewalter, S.; Lovinger, A. J.; Persoons, A. *J. Am. Chem. Soc.* **1998**, *120*, 8656.
(23) Nandi, N.; Volhardt, D. *Chem. Rev.* **2003**, *103*, 4033.
(24) Guo, Z.; Yuan, J.; Cui, Y.; Chang, F.; Sun, W.; Liu, M. *Chem.−Eur. J.* **2005**, *11*, 4155.
(25) Zhang, G.; Zhai, X.; Liu, M. *J. Phys. Chem. B* **2006**, *110*, 10455.
(26) Triulzi, R. C.; Li, C.; Naist, D.; Orbulescu, J.; Leblanc, R. M. *J. Phys. Chem. C* **2007**, *111*, 4661.
(27) Chen, P.; Ma, X.; Liu, M. *Macromolecules* **2007**, *40*, 4780.

10.1021/la801299a CCC: $40.75
Published on Web 08/08/2008

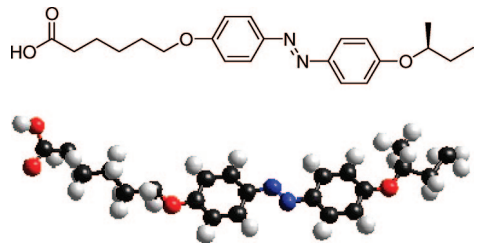

Figure 1. (Top) Chemical structure of (*S*)-4-*sec*-butyloxy-4′-[5″-(methyloxycarbonyl)pentyl-1″-oxy]azobenzene, abbreviated as AZO-C4(S). (Bottom) Molecular model that has been geometrically optimized by using the conjugated gradient Newton−Raphson algorithm in molecular mechanics (MM+ by Allinger).

azobenzene derivatives.[7,28−32] The physicochemical properties of LB films incorporating azobenzene derivatives have been related before[31,32] with structural characteristics and molecular features. However, in spite of the large body of published work on LB films incorporating azobenzene derivatives, there are few data available in the literature reporting supramolecular architectures of azobenzenes in LB films.[33]

Prompted by this picture of the current landscape, we have sought to employ the LB technique for the preparation of oriented molecular films of a chiral azobenzene derivative. Specifically, we report the synthesis of (*S*)-4-*sec*-butyloxy-4′-[5″-(methyloxycarbonyl)pentyl-1″-oxy]azobenzene, abbreviated as AZO-C4(S) (Figure 1), the Langmuir- and LB-film-forming behavior of this compound, and a characterization of the resulting films. The compound AZO-C4(S) features a polar carboxylic end group, which facilitates the spreading of the molecule as well as its anchoring onto the water surface. The alkyl chains together with the hydrophobic azobenzene core prevent AZO-C4(S) molecules from being dissolved in water and provide stability to the monolayer thanks to lateral $\pi-\pi$ and van der Waals interactions with neighboring molecules. The structures of the molecule and the chiral group were specifically designed to produce chiral supramolecular LB films. The detailed organization of AZO-C4(S) molecules within Langmuir monolayers, the formation of a supramolecular architecture at the air−water interface for high surface pressures, and the final organization of AZO-C4(S) molecules in LB films and their supramolecular chirality have been thoroughly studied by microscopic, optical, and spectroscopic procedures.

Experimental Section

Synthesis of Materials. *(S)-4-sec-Butyloxynitrobenzene (***1***).* (*R*)-(−)-2-Butanol (10.00 g, 134.90 mmol), *p*-nitrophenol (18.77 g, 134.90 mmol), and diisopropylazadicarboxylate (27.28 g, 134.90 mmol) were dissolved in dry THF (100 mL) under an Ar atmosphere and cooled in a water−ice bath. Then, a solution of triphenylphosphine (35.38 g, 134.90 mmol) in 50 mL of dry THF was added dropwise with stirring. The mixture was stirred at room temperature overnight, the precipitate was filtered off, and the solution was washed twice with a saturated Na_2CO_3 solution, twice with water, and then with brine. The organic phase was dried, concentrated, and purified by flash chromatography using hexane/ethyl acetate (8:2) as an eluent to yield the desired compound as a viscous yellowish oil. Yield: 24.70 g (126.50 mmol, 94%).

^{1}H NMR (400 MHz, $CDCl_3$, δ): 8.12 (d, $J = 9.3$ Hz, 2H), 6.88 (d, $J = 9.3$ Hz, 2H), 4.44−4.34 (m, 1H), 1.82−1.55 (m, 2H), 1.29 (d, $J = 6.1$ Hz, 3H), 0.94 (t, $J = 7.5$ Hz, 3H). ^{13}C NMR (100 MHz, $CDCl_3$, δ): 163.42, 140.76, 125.73, 115.02, 75.82, 28.80, 18.76, 9.41. IR (Nujol, cm^{-1}): 2975, 2937, 2880, 1605, 1593, 1512, 1495, 1342, 1262, 1110, 847.

*(S)-4-sec-Butyloxyaniline (***2***).* Hidrazyne monohydrate (98%, 3.00 mL, 61.85 mmol) was added dropwise to a solution of 6.00 g (30.73 mmol) of the nitrobenzene derivative in 60 mL of ethanol. After the solution was heated to 40 °C, 1.50 g of activated Raney nickel was added in portions until no further reaction was observed. The resulting mixture was filtered off of the Raney nickel, and the ethanol was removed under reduced pressure. The crude was dissolved in 60 mL of diethylether, washed with water and brine, and dried with anhydrous $MgSO_4$. The solvent was distilled off, giving the product aniline as a yellow oil that was used without further purification. Yield: 4.60 g (27.84 mmol, 91%).

^{1}H NMR (400 MHz, $CDCl_3$, δ): 6.74 (d, $J = 8.7$ Hz, 2H), 6.63 (d, $J = 8.7$ Hz, 2H), 4.15−4.07 (m, 1H), 3.53−3.17 (s broad, 2H), 1.77−1.50 (m, 2H), 1.24 (d, $J = 6.1$, 3H), 0.97 (t, $J = 7.4$, 3H). ^{13}C NMR (100 MHz, $CDCl_3$, δ): 151.20, 140.15, 117.90, 116.38, 76.41, 29.24, 19.40, 9.88. IR (Nujol, cm^{-1}): 3428, 3355, 3219, 2969, 2921, 2877, 1607, 1541, 1509, 1464, 1233.

*(S)-4-sec-Butyloxy -4′-hydroxyazobenzene (***3***).* A 2.5 M $NaNO_2$ solution (6.20 mL, 15.50 mmol) was added dropwise at a temperature below 5 °C to a heterogeneous mixture of 2.54 g (15.37 mmol) of aniline derivative **2** in 8 mL of 5 M HCl. The mixture was held at 5 °C and added carefully to a solution of 1.45 g (15.37 mmol) of phenol in 15.00 mL of 2 M NaOH. The product precipitated upon addition of NaCl. It was collected with a Büchner funnel and purified by flash chromatography using dichloromethane as an eluent to yield the required product as yellow-orange crystalline leaflets. Yield: 3.00 g (11.10 mmol, 72%).

^{1}H NMR (400 MHz, $CDCl_3$, δ): 7.89 (d, $J = 9.0$ Hz, 2H), 7.82 (d, $J = 8.8$ Hz, 2H), 7.00 (d, $J = 9.0$, 2H), 6.88 (d, $J = 8.8$, 2H), 4.44−4.34 (m, 1H), 1.86−1.60 (m, 2H), 1.34 (d, $J = 6.1$, 3H), 1.00 (t, $J = 7.5$, 3H). ^{13}C NMR (100 MHz, $CDCl_3$, δ): 160.38, 158.20, 146.88, 146.56, 124.50, 124.34, 115.91, 115.80, 75.37, 29.14, 19.16, 9.71. IR (KBr, cm^{-1}): 3380 (broad), 2972, 2933, 1596, 1499, 1249, 1147, 842.

*(S)-4-sec-Butyloxy -4′-[5″-(methyloxycarbonyl)pentyl-1″-oxy]azobenzene (***4***).* A mixture of 18-crown-6 (0.40 g, 1.51 mmol), finely ground potassium carbonate (4.60 g, 33.28 mmol), (*S*)-4-*sec*-butyloxy-4′-hydroxyazobenzene (5.00 g, 18.50 mmol), and methyl-6-bromohexanoate (4.30 g, 20.57 mmol) in acetone (100 mL) was stirred vigorously and heated under reflux for 24 h. The mixture was filtered and concentrated in vacuo. The crude product was recrystallized from methanol, yielding the required compound as an orange solid. Yield: 6.90 g (17.31 mmol, 94%).

^{1}H NMR (400 MHz, $CDCl_3$, δ): 7.86 (dd, $J = 8.9$, 2.0 Hz, 4H), 6.97 (dd, $J = 8.9$, 0.8 Hz, 4H), 4.44−4.35 (m, 1H), 4.03 (t, $J = 6.4$ Hz, 2H), 3.68 (s, 3H), 2.36 (t, $J = 7.5$ Hz, 2H), 1.90−1.45 (m, 8H), 1.34 (d, $J = 6.1$ Hz, 3H), 1.00 (t, $J = 7.5$ Hz, 3H). ^{13}C NMR (100 MHz, $CDCl_3$, δ): 174.0, 161.0, 160.4, 146.8, 146.6, 124.4, 124.3, 115.8, 114.6, 75.3, 70.1, 51.5, 33.9, 29.1, 28.9, 25.6, 24.7, 19.2, 9.7. IR (KBr, cm^{-1}): 2922, 2855, 1738, 1597, 1577, 1496, 1452, 1244.

(S)-4-sec-Butyloxy-4′-[5″-(hydroxycarbonyl)pentyl-1″-oxy]azobenzene AZO-C4(S). Compound **4** (7.20 g, 18.07 mmol) was added to a sodium hydroxide solution (90.00 mL, 3 M). THF (14.00 mL) was then added until a homogeneous suspension was formed. The reaction mixture was stirred at room temperature for 4 days, during which the reaction was monitored with TLC. On complete hydrolysis, the suspension was neutralized with a solution of hydrochloric acid (5 M) at 0 °C. This furnished the crude product as an orange solid that was filtered off and washed with acetone. The crude product was recrystallized twice from ethanol to yield the desired acid. Yield: 4.70 g (12.22 mmol, 68%).

^{1}H NMR (400 MHz, DMSO-d_6, δ): 7.81 (dd, $J = 9.0$, 2.3 Hz, 4H), 7.08 (dd, $J = 9.0$, 3.8 Hz, 4H), 4.56−4.47 (m, 1H), 4.06 (t,

(28) Matsumoto, M.; Miyazaki, D.; Tanaka, M.; Azumi, R.; Manda, E.; Kondo, Y.; Yoshino, N.; Tachibana, H. *J. Am. Chem. Soc.* **1998**, *120*, 1479.
(29) Matsumoto, M.; Terrettaz, S.; Tachibana, H. *Adv. Colloid Interface Sci.* **2000**, *87*, 147.
(30) Ichimura, K.; Han, M. *Chem. Lett.* **2000**, 286.
(31) Haro, M.; Giner, B.; Gascón, I.; Royo, F. M.; López, M. C. *Macromolecules* **2007**, *40*, 2058.
(32) Haro, M.; Villares, A.; Gascón, I.; Artigas, H.; Cea, P.; López, M. C. *Electrochim. Acta* **2007**, *52*, 5086.
(33) Zhang, Y.; Chen, P.; Liu, M. *Langmuir* **2006**, *22*, 10246.

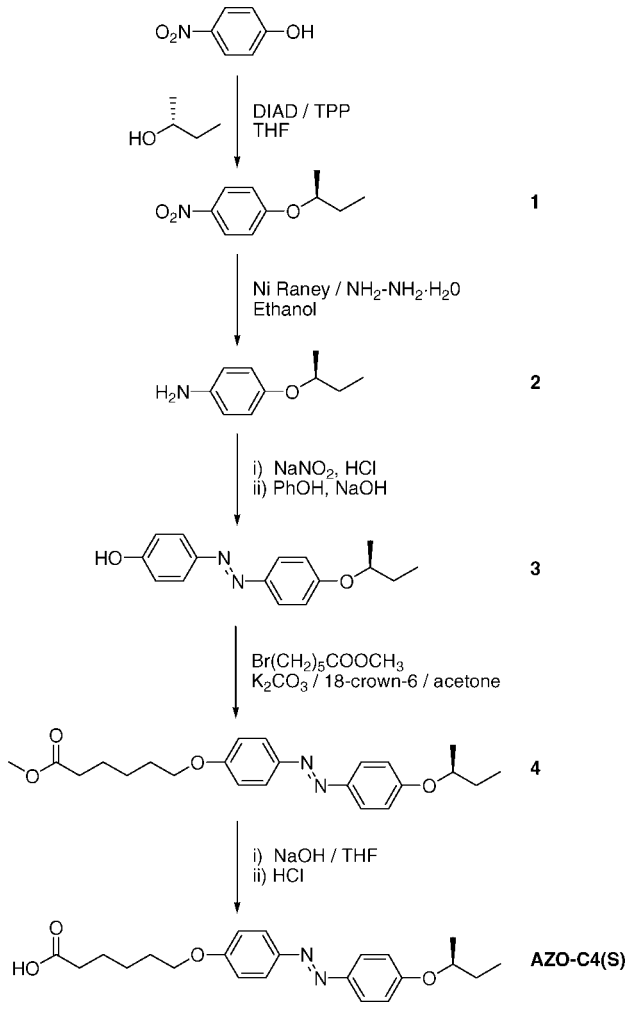

Figure 2. Synthesis of azobenzene chromophore AZO-C4(S).

$J = 6.4$ Hz, 2H), 2.24 (t, $J = 7.3$ Hz, 2H), 1.81−1.38 (m, 8H), 1.27 (d, $J = 6.0$ Hz, 3H), 0.94 (t, $J = 7.4$ Hz, 3H). ^{13}C NMR (100 MHz, DMSO-d_6, δ): 174.4, 160.8, 160.0, 146.0, 145.8, 124.1, 124.0, 115.8, 114.8, 74.5, 67.7, 33.5, 28.4, 28.3, 25.04, 24.19, 18.9, 9.4. IR (KBr, cm^{-1}): 3462 (broad), 2969, 2941, 2872, 1706, 1600, 1579, 1498, 1316, 1243, 1147, 845.

Film Fabrication. Langmuir films were prepared on a NIMA Teflon trough with dimensions of 720 × 100 mm^2; the trough was housed in a constant-temperature clean room (20 ± 1 °C). The surface pressure (π) of the monolayers was measured with a Wilhelmy paper plate pressure sensor. The subphase was water (Millipore Milli-Q, resistivity 18.2 MΩ·cm). AZO-C4(S) was dissolved in HPLC-grade chloroform (99.9%) provided by Aldrich. To construct the LB films, we delivered a 5×10^{-5} M solution of AZO-C4(S) in chloroform from a syringe held very close to the surface, allowing the surface pressure to return to a value as close as possible to zero between each addition. The solvent was allowed to evaporate completely over a period of at least 15 min before compression of the monolayer commenced at a constant sweeping speed of 1.1×10^{-2} nm^2 molecule^{-1} min^{-1}. The ΔV−A measurements were recorded using a Kelvin probe provided by Nanofilm Technologie GmbH, Göttingen, Germany. Monolayer formation was monitored by Brewster angle microscopy using a mini-BAM from Nanofilm Technologie GmH. A commercial UV−vis reflection spectrophotometer, described elsewhere,[34] was used to obtain the reflection spectra of the Langmuir films during the compression process.

The LB films were fabricated by the vertical dipping method with a dipping speed of 6 mm min^{-1}. Depending on the nature of the experiment, several solid substrates were employed: quartz (UV−vis and circular dichroism, CD, spectroscopy); CaF_2 (infrared, IR, spectroscopy); and mica (atomic force microscopy, AFM). More details concerning the cleaning procedure of the substrates and the preparation conditions have been reported before.[35,36] UV−vis absorption spectra of the LB films were acquired on a Varian Cary 50 UV−visible spectrophotometer. The IR transmission spectra were recorded with a Jasco 410 Fourier transform infrared spectrometer. The AFM experiments were performed by means of a multimode extended microscope with Nanoscope IIIA electronics from Digital Instruments operating in the ambient atmosphere. The AFM tip was made of silicon with a resonance frequency of 285 kHz and a force constant of 42 N m^{-1}. All images were recorded at room temperature using tapping mode. The scanning rate was 1 Hz, and the amplitude set point was lower than 1 V. CD spectra were measured using a Jasco J-710 spectropolarimeter. The LB films deposited onto quartz were placed in a rotating holder around the light beam, and CD spectra were registered every 60° while checking that in all cases the CD spectrum remained unaltered and the contribution of linear dichroism to the CD spectra was negligible.

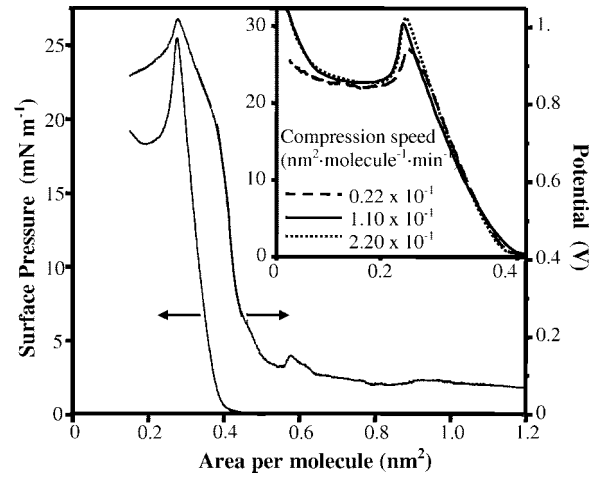

Figure 3. π−A (−) and ΔV−A (---) isotherms of AZO-C4(S) recorded at a compression speed of 1.1×10^{-2} nm^2·molecule^{-1}·min^{-1}. The inset graph shows π−A isotherms of AZO-C4(S) at the indicated compression speeds expressed in nm^2·molecule^{-1}·min^{-1}.

Results and Discussion

Synthesis of the Chromophore. The azobenzene chromophore was synthesized according to the synthetic pathway shown in Figure 2. The azobenzene was prepared by an azo coupling reaction of sodium phenoxide and **2**, which was prepared from 4-nitrophenol by etherification with (*R*)-1-methylpropanol and further reduction of the nitro group. The carboxylic-ended aliphatic chain was introduced by a Williamson reaction and subsequent hydrolysis of the ester group to yield AZO-C4(S). This monomer has a calamitic structure, but no mesomorphic properties were observed when it was studied by polarizing optical microscopy and differential scanning calorimetry (DSC).

Langmuir Films. The surface pressure (π) and the surface potential (ΔV) versus the area per molecule (A) isotherms of AZO-C4(S) are shown in Figure 3. The takeoff in the ΔV−A isotherm takes place at ca. 0.55 nm^2·molecule^{-1}, and the takeoff in the π−A isotherm occurs over an area of 0.45 nm^2·molecule^{-1}. This is in agreement with the well-known fact that phase transitions are detected a few squared Ångstroms earlier in ΔV−A

(34) Cea, P.; Martín, S.; Villares, A.; Möbius, D.; López, M. C. *J. Phys. Chem. B* **2006**, *110*, 963.

(35) Cea, P.; Morand, J. P.; Urieta, J. S.; López, M. C.; Royo, F. M. *Langmuir* **1996**, *12*, 1541.

(36) Martín, S.; Cea, P.; Lafuente, C.; Royo, F. M.; López, M. C. *Surf. Sci.* **2004**, *563*, 27.

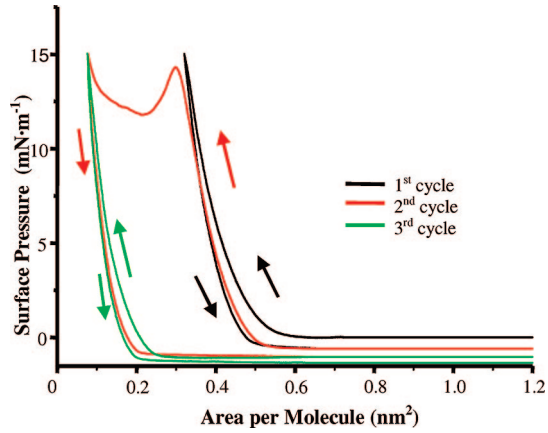

Figure 4. Compression−expansion cycles of an AZO-C4(S) monolayer recorded at a compression speed of 1.1×10^{-2} nm^2·molecule^{-1}·min^{-1}.

isotherms.[37−39] Compression of the AZO-C4(S) monolayer results in an increase in the surface pressure and surface potential followed by an overshoot for an area of ca. 0.28 nm^2·molecule^{-1} in the $\pi-A$ isotherm. This area per molecule is in good agreement with values previously reported for the collapse of azobenzene monolayers, which are around 0.3 nm^2.[40−42] In addition, the theoretical area per azobenzene unit with an orientation of the transition dipole moment normal to the water surface is 0.245 nm^2.[43] These data are consistent with the overshoot being caused by the collapse of the monolayer. The influence of the compression speed on the overshoot is illustrated in the inset of Figure 3. Although the isotherms' profile is not modified, a dependence of the overshoot surface pressure on the compression speed is clearly observed, which is indicative of a kinetic effect. A further compression process is followed by a new increase in the surface pressure.

To provide deeper insight into the origin of the overshoot, the behavior of the $\pi-A$ isotherm during repeated cycles of compression and expansion was examined (Figure 4). In the first cycle, when the barrier direction is reversed at 15 mN·m^{-1}, a relatively small hysteresis effect occurs. In the second cycle, the surface pressure increases until an overshoot at 14.3 mN·m^{-1} is reached, which is accompanied by a large hysteresis effect, suggesting that the overshoot involves some kind of irreversible process. The overshoot appears at a considerable lower surface pressure in the second cycle in comparison with the first one (Figure 3). Such a phenomenon might be explained by assuming that some nucleation domains are formed in the first compression cycle. These nucleation points may favor the appearance of the overshoot at a lower surface pressure in the second compression process. In the third compression−expansion cycle, the $\pi-A$ isotherm for the compression process practically overlays the expansion $\pi-A$ curve of the second cycle, which is consistent with the overshoot being caused by some kind of irreversible process. The third cycle hardly shows any hysteresis effect. Further compression−expansion cycles lead to $\pi-A$ graphs that overlay the isotherm for the third cycle. It is noteworthy that for a certain surface pressure the area per molecule in the $\pi-A$ curve for the first cycle is 3 times larger than the area per molecule in $\pi-A$ graphs recorded when the overshoot was passed (third and consecutive cycles). This result indicates that the origin of the overshot in the $\pi-A$ isotherm could be the collapse of the monolayer into a trilayer structure.[44−47] We will see later that other experimental data (reflection spectroscopy, UV−vis spectroscopy, and AFM) also lead to this conclusion.

As a complement to the information provided by the $\pi-A$ and $\Delta V-A$ isotherms, BAM images were also recorded at different stages of compression (Figure 5). At 15 mN·m^{-1}, the whole water surface is practically covered by the monolayer, and a highly homogeneous monolayer is formed at 20 mN·m^{-1}. At an area per molecule of 0.28 nm^2 (overshoot), BAM images show a significant number of bright domains or spots. Further compression results in an increase in the number, size, and brightness of these domains, suggesting that local collapses of the monolayer occur. Arguably, these local collapses lead to the formation of an ordered trilayer as $\pi-A$ isotherms suggest.

Trilayer formation and supramolecular organization in Langmuir films were investigated in situ by UV−vis reflection spectroscopy through the reflection of unpolarized light under normal incidence. Figure 6 depicts the reflection spectra recorded at different values of the area per molecule upon the compression process. The band located at ca. 250 nm is attributed to the transition dipole moment along the short axis of the azobenzene chromophore[47] (A band). The band in the 300−500 nm region is assigned to the transition dipole moment along the long axis of AZO-C4(S) (B band), which is strongly affected by the molecular environment of the azobenzene.[47] At the beginning of the compression process, the B band is centered at 354 nm. Upon compression, this band is progressively blue shifted until a value of 342 nm is reached for an area of 0.31 nm^2·molecule^{-1} (just before the overshoot), which is consistent with the formation of 2D H-aggregates at the air−water interface. These aggregates are commonly found in LB films in which the chromophore has the main dipole transition moment arranged more or less along the amphiphile backbone, including other *trans*-azobenzenes,[48] *trans*-stilbenes,[49] hemicyanine derivatives,[50] squaraines,[51] and phenylene-ethynylene oligomers.[52]

When the overshoot is passed on the compression process, the spectra profile changes drastically. The two $\pi-\pi^*$ transition bands (A and B) show vibrational fine structure. The vibrational fine structure is confirmed by the close connection between the electronic and vibrational properties, as nicely exemplified by correlating the differences in energy of the consecutive vibronic peaks in the UV−vis to the wavenumbers of the Raman lines.[53] The differences in energy between two consecutive peaks in the AZO-C4(S) reflection spectrum are 1429 cm^{-1} (between 373

(37) Villares, A.; Lydon, D. P.; Porrès, L.; Beeby, A.; Low, P. J.; Cea, P.; Royo, F. M. *J. Phys. Chem. B* **2007**, *111*, 7201.
(38) Oliveira, O. N., Jr.; Bonardi, C. *Langmuir* **1997**, *13*, 5920.
(39) Pera, G.; Villares, A.; López, M. C.; Cea, P.; Lydon, D. P.; Low, P. J. *Chem. Mater.* **2007**, *19*, 857.
(40) Freimanis, J.; Markava, E.; Matisova, G.; Gerca, L.; Muzikante, I.; Rutkis, M.; Silinsh, E. *Langmuir* **1994**, *10*, 3311.
(41) Maack, J.; Ahuja, R. C.; Tachibana, H. *J. Phys. Chem.* **1995**, *99*, 9210.
(42) Engelking, J.; Wittemann, M.; Rehahn, M.; Menzel, H. *Langmuir* **2000**, *16*, 3407.
(43) Pedrosa, J. M.; Martín-Romero, M. T.; Camacho, L. *J. Phys. Chem. B* **2002**, *106*, 2583.
(44) Balogh, D. T.; Dhanabalan, A.; Dynarowicz-Latka, P.; Schenning, A. P. H. J.; Oliveira Jr, O. N.; Meijer, E. W.; Janssen, R. A. J. *Langmuir* **2001**, *17*, 3281.
(45) Cea, P.; Lafuente, C.; Urieta, J. S.; López, M. C.; Royo, F. M. *Langmuir* **1996**, *12*, 5881.
(46) McFate, C.; Ward, D.; Olmsted, J. I. *Langmuir* **1993**, *9*, 1036.
(47) Kajiyama, T.; Aizawa, M. *New Developments in Construction and Functions of Organic Thin Films*; Elsevier: 1996; Vol. *4*.
(48) Pedrosa, J. M.; Martín, M. T.; Camacho, L.; Möbius, D. *J. Phys. Chem. B* **2002**, *106*, 2583.
(49) Martin, S.; Cea, P.; Pera, G.; Haro, M.; López, M. C. *J. Colloid Interface Sci.* **2007**, *308*, 239.
(50) Heeseman, J. *J. Am. Chem. Soc.* **1980**, *102*, 2166.
(51) Chen, H.; Law, K.-Y.; Whitten, D. G. *J. Phys. Chem.* **1996**, *100*, 5949.
(52) Villares, A.; Lydon, D. P.; Low, P. J.; Robinson, B. J.; Ashwell, G. J.; Royo, F. M.; Cea, P. *Chem. Mater.* **2008**, *20*, 258.
(53) Lanata, M.; Bertarelli, C.; Gallazi, M. C.; Bianco, A.; Del Zoppo, M.; Zerbi, G. *Chem. Phys. Lett.* **2003**, *377*, 243.

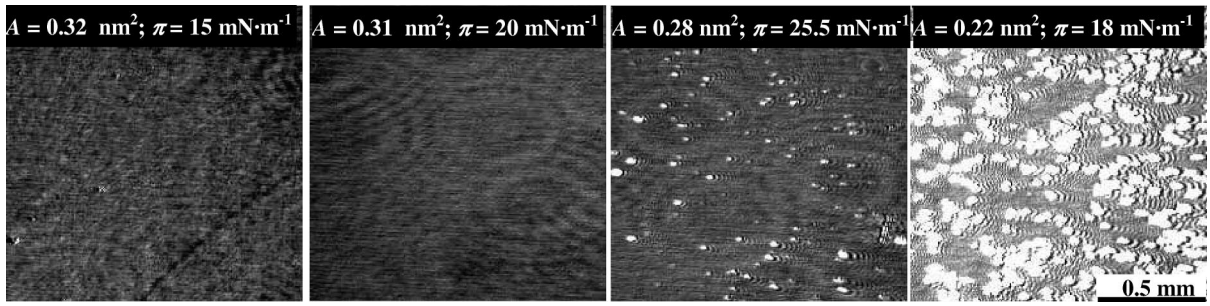

Figure 5. BAM images recorded upon the compression process at the indicated surface pressures and areas per molecule.

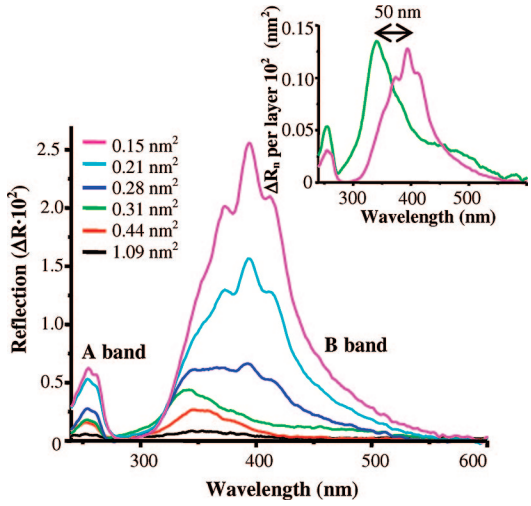

Figure 6. Reflection spectra (ΔR) recorded at the indicated area per AZO-C4(S) molecule. The inset shows the normalized reflection spectra (ΔR_n) per AZO-C4(S) layer.

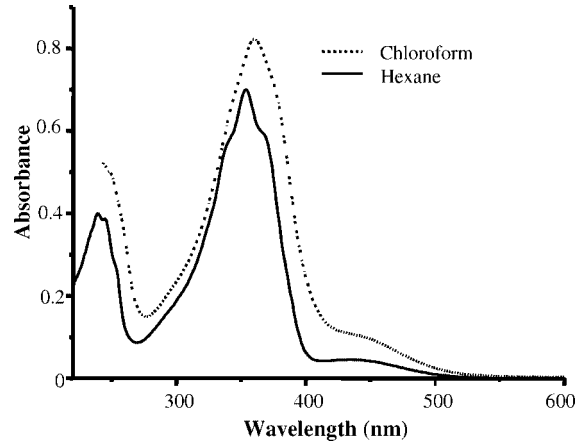

Figure 7. UV−vis spectra of AZO-C4(S) in chloroform and hexane solution.

and 394 nm) and 1109 cm^{-1} (between 394 and 412 nm). These two bands coincide, within experimental error, with the strongest characteristic azobenzene bands of the Raman spectrum reported elsewhere,[54] which have been assigned to the N=N stretching mode and in-plane C−H bending with the C−N stretching contribution, respectively. In addition, the B band is red shifted by 50 nm with respect to the spectra recorded before the overshoot, whereas the A band position remains unchanged. Such a bathochromic shift may be interpreted in terms of the formation of J aggregates (i.e., head to tail aggregates[55]). The B band also shows a shoulder around 355 nm that may correspond to isolated AZO-C4(S) molecules. The drastic change in the optical properties of the film after the overshoot is a clear indication of the achievement of a new supramolecular architecture. The reflection spectrum recorded on the first compression process at an area per molecule of 0.28 nm^2, in which the monolayer is on the verge of the overshoot, is a combination of the spectra recorded before and after the overshoot. This result is further confirmation of the overshoot in the $\pi-A$ isotherm being caused by a transition between two different molecular arrangements.

Quantitative analysis of the reflection spectra leads to other evidence of trilayer formation after the overshoot. The inset of Figure 6 shows the normalized reflection per AZO-C4(S) layer defined as $\Delta R_{n\ per\ layer}$ = (1/number of layers) × ΔR × area per molecule. Thus, the green line shows the reflection spectrum for the monolayer (number of layers = 1) before the overshoot (0.31 $nm^2 \cdot molecule^{-1}$). The magenta spectrum corresponds to the normalized reflection for a film at the air−water interface recorded at 20 $mN \cdot m^{-1}$ once the overshoot was passed on the compression process (0.15 $nm^2 \cdot molecule^{-1}$). The normalization was done assuming that the effective path length of the surface corresponds to a trilayer (i.e., in the inset of Figure 6 the magenta spectrum was calculated as $\Delta R_{n\ per\ layer} = (1/3) \times \Delta R \cdot \times$ area per molecule. The two normalized reflection spectra in the inset of Figure 6 have very similar intensities, which is consistent with the hypothesis of trilayer formation at the air−water interface.

The vibrational fine structure in azobenzene UV−vis spectra has been scarcely described in the literature.[56] In general, azobenzene molecules give unresolved bands in the UV−vis spectra probably for two reasons: (i) a considerable mixture of the $\pi-\pi^*$ and $n-\pi^*$ transitions and (ii) an overlap of the vibrational wave functions of the ground and excited states due to the change in the N=N−φ angle (where φ is the benzene group) during the excitation process.[57] However, Muniz-Miranda et al.[56] observed a vibrational fine structure in the spectrum of an azobenzene derivative in nonpolar solvent solutions that disappeared in polar media. AZO-C4(S) exhibits similar behavior, as illustrated in Figure 7, where the fine structure is observed in hexane, whereas it is not preserved in a more polar solvent such as chloroform. The fine structure in nonpolar solvents has been explained in terms of rigidification and planarization of the ground electronic state,[58] which allows conjugation between the π electrons of the N=N double bond and those of the aromatic rings. According to these data, we propose that (i) the red shift

(54) Haro, M.; Ross, D. J.; Oriol, L.; Gascón, I.; Cea, P.; López, M. C.; Aroca, R. F. *Langmuir* **2007**, *23*, 1804.
(55) McRae, E. D.; Kasha, M. *J. Chem. Phys.* **1958**, *28*, 721.
(56) Muniz-Miranda, M.; Pergolese, B.; Sbrana, G.; Bigotto, A. *J. Mol. Struct.* **2005**, *744−747*, 339.
(57) Dyck, R. H.; McClure, D. S. *J. Chem. Phys.* **1962**, *36*, 2326.
(58) Casado, J.; Zgierski, M. Z.; Ewbank, P. C.; Burand, M. W.; Janzen, D. E.; Mann, K. R.; Pappenfus, T. M.; Berlin, A.; Pérez-Inestrosa, E.; Ponze, R.; López, J. T. *J. Am. Chem. Soc.* **2006**, *128*, 10134.

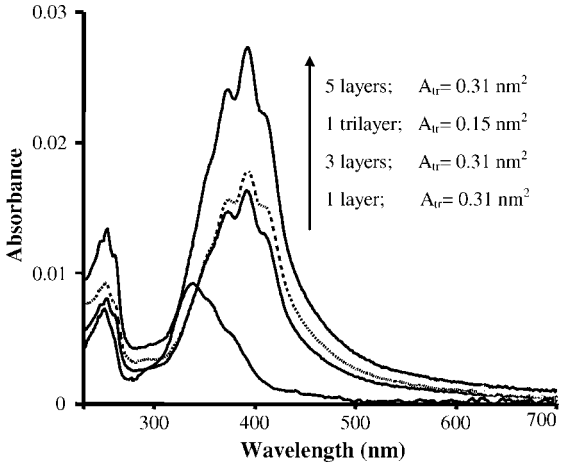

Figure 8. UV−vis spectra of one- three-, and five-layer LB films, transferred before the overshoot at 20 mN·m^{-1} (−) and one transference of the trilayer formed at the air−water interface after the overshoot at 20 mN·m^{-1} (---).

of the B band in the reflection spectra after the overshoot is due to the formation of J aggregates between molecules in adjacent layers and (ii) $\pi-\pi$ interactions between azobenzene moieties in neighboring layers may force the rigidification and planarization of the chromophore, which could explain the vibrational fine structure in the reflection spectra of AZO-C4(S) after the collapse of the monolayer into a trilayer structure.

Langmuir−Blodgett Films. Langmuir monolayers of AZO-C4(S) were transferred onto quartz substrates at 20 mN·m^{-1} (before the overshoot) and characterized by UV−vis absorption spectroscopy. The deposition was Y-type with a transference ratio of 0.8. The relationship between the absorbance and the number of layers was found to be linear up to 15 transferences. This linear relationship indicates a constant transfer ratio during the deposition and a constant architecture in the LB films.

Figure 8 shows the UV−vis spectra of the AZO-C4(S) LB films of one, three, and five layers transferred at a surface pressure of 20 mN/m (before the overshoot). The UV−vis spectrum of the one-layer LB film transferred before the overshoot shows two broad unresolved bands centered at 250 and 339 nm. On the contrary, multilayered films (three and five layers) show a red shift of the B band and vibrational fine structure for the two $\pi-\pi^*$ transition bands, which is in agreement with the fine structure being caused by the achievement of a different supramolecular architecture in multilayered films. The UV−vis spectrum of an LB film obtained by the withdrawal of the quartz substrate at 20 mN·m^{-1}, when the overshoot is passed, is also shown in Figure 8. The shape and absorbance of this spectrum is almost equal to the spectrum of the three-layer LB film when the transferences are performed before the overshoot. This result suggests that the trilayer formed at the air−water interface may be transferred to a substrate, and this trilayer has similar architecture to that of the three-layer LB film obtained by the successive transference of three monolayers. These results indicate that the supramolecular structure is due to the interactions between molecules in neighboring layers forming the multilayered film, which may be obtained either by the transference of a trilayer from the air−water interface to the solid substrate or by the transference of three monolayers.

Figure 9 shows the FTIR spectra of AZO-C4(S) in a KBr pellet and assembled in a 15-layer LB film transferred at 20 mN·m^{-1} (before the collapse into a trilayer structure) onto a CaF_2 substrate. Table 1 shows the assignment of the most significant bands in the spectra. The relative intensities of the

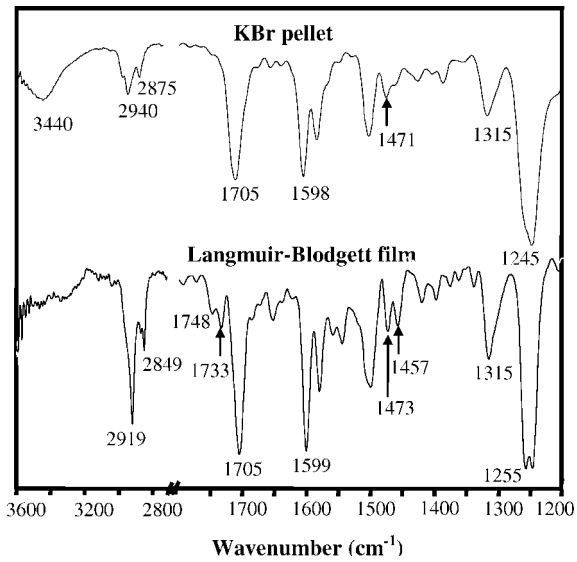

Figure 9. IR spectra of AZO-C4(S) in a KBr pellet and in a 15-layer LB film transferred at 20 mN·m^{-1} (before the collapse into a trilayer structure).

Table 1. Band Positions and Assignments for FTIR Spectra of AZO-C4(S) in a KBr Pellet and in a 15-Layer LB Film

band position (cm^{-1})KBr pellet	band position (cm^{-1})LB film	assignment
3440	∼3400	ν(O−H)
2940	2919	ν_a(C−H) alkyl chain
2875	2849	ν_s(C−H) alkyl chain
	1748	ν_a(C═O) free carboxylic group
	1733	ν_a(C═O) H-bonded carboxylic group
1705	1705	ν_a(C═O) double H-bonded carboxylic group
1598	1599	ν(C═C) aromatic group + ν(N═N)
1577	1577	ν(C═C) aromatic group + ν(N═N)
1471	1473, 1457	$\delta(CH_2)$ alkyl chain
1315	1315	β(H−C−H) alkyl chain
1245	1255	ν(C−O) ether group

bands change from the KBr pellet to the LB film, which is attributable to orientation effects in the LB film. A remarkable difference between the LB film and KBr pellet spectra is related to the C═O stretching region. It is well known that the free C═O stretching vibration of an acid group appears at around 1740 cm^{-1} and shifts to lower wavenumbers when H bonds are formed.[59] The C═O stretching vibration appears at 1705 cm^{-1} in the spectrum of AZO-C4(S) in the KBr pellet, which can be assigned to double-H-bonded COOH groups.[60] The FTIR spectrum of the LB film shows a band at 1748 cm^{-1} and another one at 1733 cm^{-1}. These two bands may correspond to the free and single-H-bonded group, respectively. The spectrum of AZO-C4(S) in the KBr pellet exhibits a strong, broad band at 3400 cm^{-1} that is assigned to the O−H stretching mode. However, this band is much weaker in the LB film, indicating a nearly perpendicular arrangement of the O−H bond with respect to the substrate plane.[35]

The FTIR spectrum of the LB film also gives important information about the conformational order and packing of the alkyl chains. When the alkyl chains are highly ordered (trans zigzag conformation), the $\nu_a(CH_2)$ and $\nu_s(CH_2)$ bands appear

(59) Silverstein, R. M.; Clayton Bassler, G.; Morril, T. C. *Spectrometric Identification of Organic Compounds*, 5th ed.; John Wiley & Sons: New York, 1991.

(60) Brauner, J. W.; Flach, C. R.; Xu, Z.; Bi, X.; Lewis, R. N. A. H.; McElhaney, R. N.; Gericke, A.; Mendelsohn, R. *J. Phys. Chem. B* **2003**, *107*, 7202.

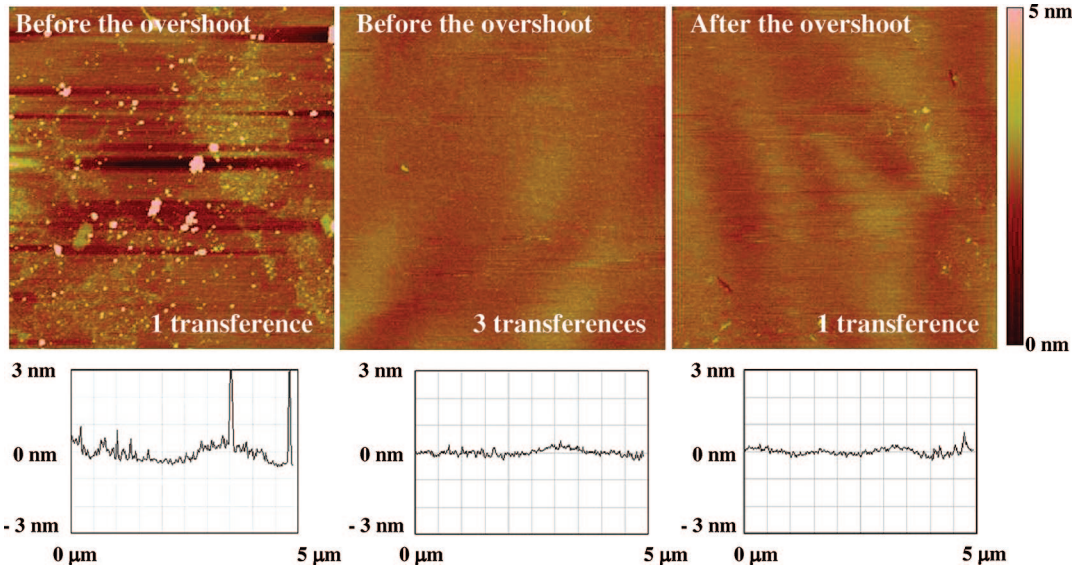

Figure 10. AFM top view ($5 \times 5\ \mu m^2$) and section analysis of AZO-C4(S) LB films of 1 (a) and 3 (b) layers transferred onto mica before the overshoot at 20 $mN \cdot m^{-1}$ and one transference (c) after the overshoot at 20 $mN \cdot m^{-1}$.

near 2918 and 2850 cm^{-1}, respectively,[61,62] whereas if conformational disorder is included in the chain, then these diagnostic bands shift to higher wavenumbers depending on the content of gauche conformations. The hydrocarbon tails in the LB film here reported present bands at 2919 and 2849 cm^{-1} that are indicative of well-ordered alkyl chains with a trans zigzag conformation.[45,63] In contrast, the spectrum of this material obtained from a KBr pellet exhibits $\nu_a(CH_2)$ and $\nu_s(CH_2)$ bands at 2940 and 2875 cm^{-1}, respectively, indicating the more random orientation of the alkyl chains. In the FTIR spectrum of the LB film, the splitting of the $\delta(CH_2)$ band occurs (1473 and 1457 cm^{-1}), indicating orthorhombic subcell packing with two molecules in one unit cell.[64−66]

The surface morphology of the films was investigated by AFM. Figure 10 shows three representative images of one- and three-layer LB films transferred onto freshly cleaved mica at 20 $mN \cdot m^{-1}$ (before the collapse into the trilayer structure) and one film transferred at 20 $mN \cdot m^{-1}$ (after the collapse). The monolayer transferred before the collapse shows 3D defects and a relatively high rms (root-mean-square) roughness of 1.29 nm. In contrast, multilayered films are very homogeneous, with rms roughness values of 0.15 nm for the three-layer LB film and 0.17 nm for the film transferred after the overshoot (trilayer). To ensure the veracity of these results, the experiments were repeated three times to obtain reproducible results. The presence of 3D defects in the one-layer LB film is likely related to the reorganization of the molecules in the film toward an energetically more favorable molecular distribution. This hypothesis is corroborated by the evolution in air observed in the UV−vis spectrum of a one-layer LB film as illustrated in Figure 11. The pristine film shows a maximum absorbance at 339 nm. This band is progressively red shifted with time, which may indicate the formation of J aggregates, arguably in a 3D arrangement as suggested by the AFM images. In contrast, the lack of 3D defects in multilayered films is indicative of a more stable arrangement of the molecules.

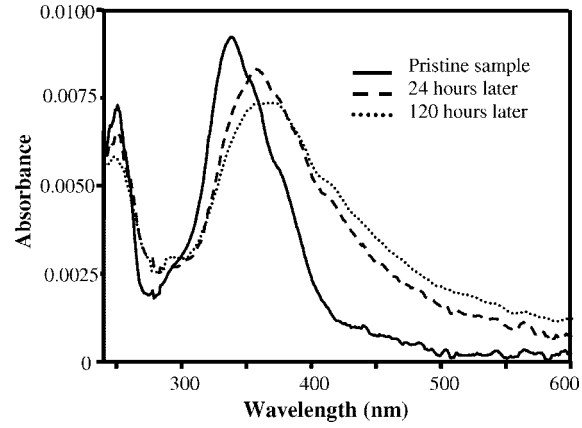

Figure 11. UV−vis spectra of a one-layer LB film transferred before the overshoot at 20 $mN \cdot m^{-1}$ and after its evolution at air, 24 and 120 h after the transference of the film.

The film thicknesses were determined by scratching the films with the AFM tip, yielding values of 2.3 nm for the one-layer LB film transferred at 20 $mN \cdot m^{-1}$ before the collapse of the film into a trilayer structure. When the height of AZO-C4(S) in a vertical position (2.4 nm) is taken into account, this film thickness corresponds to a tilt angle of the molecules of ca. 73°. The height of a three-layer LB film transferred at 20 $mN \cdot m^{-1}$ is ca. 5.8 nm. On the basis of these results together with the above presented ones (H-bonds between carboxylic acid groups, J aggregates, and fine vibrational structure in the UV−vis spectra), a schematic model for the molecular organization in the LB films is depicted in Figure 12. We propose that molecules in the second layer are inserted ca. 1 nm into the first layer, which favors the formation of J aggregates between the azobenzene chromophores in the first and second layers and might contribute to the rigidification of the azobenzene moieties. Molecules in the second and third layers interact with each other by H bonds. In addition, the linear relationship between the absorbance and the number of layers when monolayers are transferred onto quartz substrates suggests that molecules in the first, second, and third layers have a similar tilt angle.

(61) Porter, M. D.; Bright, T. B.; Allara, D. L.; Chidsey, C. E. D. *J. Am. Chem. Soc.* **1987**, *109*, 3559.
(62) Byrd, H.; Whipps, S.; Pike, J. K.; Ma, J.; Nagler, S. E.; Talham, D. R. *J. Am. Chem. Soc.* **1994**, *1994*, 295.
(63) Tang, X.; Schneider, P. B.; Buttry, D. A. *Langmuir* **1994**, *10*, 2235.
(64) Sapper. H; Cameron, D. G.; H., M. H. *Can. J. Chem.* **1981**, *59*, 2543.
(65) Snyder, R. G.; Schachtschneider, J. H. *Spectrochim. Acta* **1963**, *19*, 85.
(66) Umemura, J.; Cameron, D. G.; Mantsch, H. H. *Biochim. Biophys. Acta* **1980**, *606*, 32.

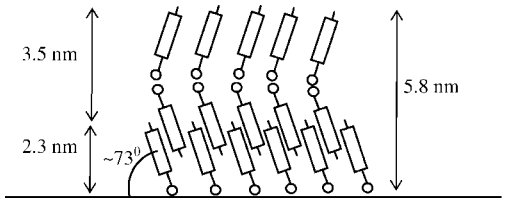

Figure 12. Schematic model for a multilayered LB film of AZO-C4(S).

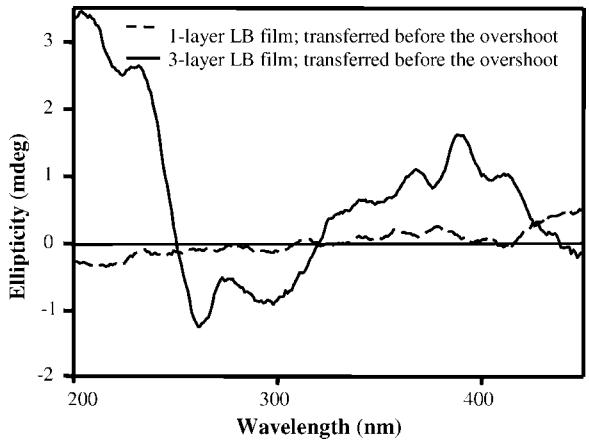

Figure 13. CD spectra of a monolayer and a three-layer LB film transferred before the collapse of the monolayer into a trilayer structure.

We have used CD spectroscopy to investigate in more detail the supramolecular architecture of the films and their optical activity. One-layer LB films do not show any CD signal (Figure 13). In contrast, a significant CD response is observed for a three-layer LB film as illustrated in Figure 13. An identical CD spectrum has been obtained for a film fabricated by the transference of a trilayer formed at the air−water interface. This result indicates that chiro-optical activity in LB films is the result of an ordered multilayered supramolecular architecture.

The low-wavelength region of the spectra is characterized by a split Cotton effect (SCE), with two minima at 262 and 299 nm, consistent with the coupling[67] of two or more azobenzene $\pi-\pi^*$ dipolar transition moments along the short axis of the molecule (responsible for the A band in the UV−vis spectrum). Similar split Cotton effects have been reported for polypeptides and interpreted in terms of an α-helical conformation,[68,69] whereas one negative peak has been assigned to molecules arranged in beta planar structures.[70,71] These observations are in agreement with supramolecular architecture in which the plane that contains the azobenzene moiety rotates from one layer to the next one, with the rotation of the $\pi-\pi^*$ dipolar transition moment along the short azobenzene axis drawing a helix. In the 350−450 nm region of the spectrum, a positive Cotton effect (CE) exhibiting fine vibrational structure is observed (Figure 13). This band can be assigned to the $\pi-\pi^*$ transition of the dipole moment along the long azobenzene axis (B band in the UV−vis spectrum).

(67) Berova, N.; Di Bari, L.; Pescitelli, G. *Chem. Soc. Rev.* **2007**, *36*, 914.
(68) Pieroni, O.; Fissi, A.; Popova, G. *Prog. Polym. Sci.* **1998**, *23*, 81.
(69) Sjogren, H.; Ulvenlund, S. *J. Phys. Chem. B* **2004**, *108*, 20219.
(70) Ulvenlund, S.; Gillgren, H.; Stenstam, A.; Backman, P.; Sparr, E. *J. Colloid Interface Sci.* **2001**, *242*, 346.
(71) Zheng, J.; Constantine, C.; Rastogi, V. K.; Cheng, T.-C.; DeFrank, J. J.; Leblanc, R. M. *J. Phys. Chem. B* **2004**, *108*, 17238.

Conclusions

In this contribution, we have presented the synthesis and fabrication of Langmuir and Langmuir−Blodgett films from an azobenzene chiral derivative. We have thoroughly studied the surface behavior of the azo derivative at the air−water interface by means of $\pi-A$ and $\Delta V-A$ isotherms, BAM, and UV−vis reflection spectroscopy, concluding that a reorganization of the molecules in the monolayer occurs at an area of 0.28 $nm^2 \cdot molecule^{-1}$, inducing trilayer formation. Reflection spectra of multilayered films were characterized by vibrational fine structure as well as a red shift of 50 nm with respect to monomolecular films, which was interpreted in terms of a new supramolecular architecture in the Langmuir film. The AFM revealed that the transference of one monolayer yielded non-homogeneous films with 3D defects, whereas the transference of the trilayer led to a highly ordered film. These results are consistent with an energetically more favorable molecular distribution in multilayered films. Moreover, the supramolecular architecture of trilayers at the air−water interface was transferred undisturbed onto the solid substrates whereas similar molecular architecture was achieved for multilayered LB films fabricated by the successive deposition of monolayers. FTIR and UV−vis absorption spectroscopy were consistent with the supramolecular architecture in multilayered films being induced by H bonds between molecules in neighboring layers and $\pi-\pi$ interactions between azo moieties. Multilayered LB films exhibited CD spectra with an SCE in the high-energy region of the spectra and a CE in the low-energy region. The next stage in these investigations will center on the measurement of the photoinduced birefringence of mono- and multilayered AZO-C4(S) structures and comparison with similar measurements from other azobenzene-containing polymers.

Acknowledgment. We are grateful for financial assistance from the Ministerio de Educación y Ciencia (MEC) and fondos Feder in the framework of projects CTQ2006-05236 and MAT2005-06373-C02-01. We also thank Diputación General de Aragón (DGA) for its support through interdisciplinary project PM079/2006 (P.C. and M.C.L). J.d.B. and A.V. acknowledge grants from DGA and MEC, respectively. We very much appreciate Jordi Diaz's efforts in making the AFM measurements (Scientific-Technical Services, Nanometric Techniques, Barcelona University).

LA801299A